European Heart Journal – Cardiovascular Imaging (2015) **16**, 74–80
doi:10.1093/ehjci/jeu167

Early myocardial and skeletal muscle interstitial remodelling in systemic sclerosis: insights from extracellular volume quantification using cardiovascular magnetic resonance

Andrea Barison[1,2], Luna Gargani[3], Daniele De Marchi[1], Giovanni Donato Aquaro[1], Serena Guiducci[4], Eugenio Picano[3], Marco Matucci Cerinic[4], and Alessandro Pingitore[3]*

[1]Fondazione Toscana 'Gabriele Monasterio', CNR, Regione Toscana, Pisa, Italy; [2]Institute of Life Sciences, Scuola Superiore 'Sant'Anna', Pisa, Italy; [3]Clinical Physiology Institute, National Research Council, CNR, Pisa, Italy; and [4]Department of Rheumatology, Azienda Ospedaliero-Universitaria Careggi, University of Florence, Italy

Received 5 June 2014; accepted after revision 22 July 2014; online publish-ahead-of-print 4 September 2014

Aims Systemic sclerosis (SSc) may induce cardiac fibrosis and systo-diastolic dysfunction. Cardiovascular magnetic resonance (CMR) can detect replacement myocardial fibrosis with late gadolinium enhancement (LGE) and interstitial myocardial fibrosis with T1 mapping techniques. The aim of the study was to detect subclinical cardiac involvement with CMR in paucisymptomatic SSc patients with no previous history of myocardial disease, comparing it with skeletal muscle remodelling.

Methods and results Thirty consecutive SSc patients (mean age: 51 ± 12 years, all women) and 10 healthy controls (mean age: 48 ± 15 years, all women) underwent clinical, biohumoral assessment, and CMR. Extracellular volume fraction (ECV) was calculated from pre- and post-contrast T1 values in the myocardium and skeletal muscle. Seventeen patients (57%) were asymptomatic, 13 (43%) paucisymptomatic (effort dyspnoea). All patients had normal biventricular volumes and systolic function, while LGE was present in seven patients (23%). Myocardial ECV was significantly increased in patients with SSc (30 ± 4%) than controls (28 ± 4%, $P = 0.03$), as was skeletal muscle ECV (23 ± 6% vs. 18 ± 4%, $P < 0.01$). Myocardial ECV did not differ between patients with and without LGE (P = NS) and showed no significant correlations with clinical data, biventricular volumes, systolic, or diastolic function. Overall, myocardial ECV showed a significant correlation with skeletal muscle ECV ($R = 0.58$, $P < 0.001$).

Conclusion SSc is associated not only with myocardial replacement fibrosis, as detected by LGE, but also with interstitial remodelling of the myocardium and skeletal muscles, as detected by an increased ECV also in patients with normal biventricular function, with potential diagnostic, prognostic, and therapeutic clinical implications.

Keywords Systemic sclerosis • Cardiovascular magnetic resonance • Cardiac T1 mapping • Late gadolinium enhancement • Myocardial fibrosis

Introduction

Systemic sclerosis (SSc) is a heterogeneous disease whose pathogenesis is characterized by autoimmunity, inflammation, small vessel disease, and fibroblast dysfunction, leading to increased extracellular matrix deposition.[1] SSc is present throughout the world, with variable incidence across different ethnic groups and different geographic regions, and a typical age of onset between 30 and 50 years.[2] The disease may affect the myocardium, but its involvement is often clinically under recognized and may hold poor prognosis.[3,4] In the last three decades, while the mortality rates secondary to renal crisis and to pulmonary causes have been substantially modified, those related to cardiac involvement have remained apparently unchanged at ∼15% of all SSc deaths.[5] Immunoinflammatory damage, vasospasm, ischaemia and fibrosis cause perfusion defects, diastolic dysfunction, arrhythmias and, eventually, systolic cardiac

* Corresponding author. Tel: +39 0503152605. Email: pingi@ifc.cnr.it

failure. Cardiac involvement has also been correlated to skeletal muscle involvement, where inflammatory microvasculopathy and interstitial fibrosis may occur.[6]

In SSc cardiac magnetic resonance (CMR) provides significant information, not only allowing a precise definition of biventricular and biatrial size and function, but also allowing detailed tissue characterization. Late gadolinium enhancement (LGE) is known to detect fibrosis and necrosis in ischaemic and non-ischaemic cardiomyopathies.[7,8] Heterogeneous myocardial LGE has been described in SSc patients and correlated with autopsy findings of patchy myocardial oedema and fibrosis among interspersed normal myocardium.[9,10] Several studies demonstrated a variable prevalence of LGE in SSc patients, ranging from 15 to 66%,[7,8,11–13] mostly with a mid-wall linear pattern or a nodular patchy pattern, involving the basal and mid-segments of the left ventricle: these different rates and patterns of fibrosis may be due to methodological differences among the studies and to the heterogeneity of patient populations.

On the other hand, in SSc patients, diffuse myocardial fibrosis could be missed by traditional LGE imaging, which relies on differential uptake of gadolinium in abnormal (fibrotic) vs. relatively normal (non-fibrotic) myocardium. Recent advances in CMR allow surrogate estimation of diffuse myocardial fibrosis using a T1 mapping technique: native (i.e. pre-contrast) T1 mapping is highly sensitive to myocardial water and detects myocardial oedema,[14,15] but is also sensitive to myocardial fibrosis[16]; adding post-contrast T1 mapping to pre-contrast T1 mapping acquisitions allows to calculate the gadolinium partition coefficient and the extracellular volume fraction (ECV) of the myocardium and other tissues, provided there is a steady-state equilibrium between the bloodpool and the interstitium.[17] Both pre- and post-contrast T1 mapping have been shown to correlate well with histological indices of myocardial fibrosis in various clinical contexts.[16,18,19] Myocardial T1 mapping has become a novel tool for the tissue characterization of cardiomyopathies,[20] and it has been recently applied to SSc patients, showing subtle myocardial interstitial remodelling .[21,22]

The purpose of this study in SSc patients with no previous history of cardiac disease was to assess myocardial interstitial remodelling, using a pre- and post-contrast T1 mapping CMR approach, and to correlate it with skeletal muscle interstitial remodelling.

Methods

From June 2010 to June 2011, thirty consecutive SSc patients (mean age: 51 ± 12 years, all women) and 10 healthy controls (mean age: 48 ± 15 years, all women) were prospectively enrolled in our study and underwent routine clinical, biohumoral, echocardiographic assessment, and CMR. All patients were followed up at the Department of Rheumatology of Florence (Italy) and fulfilled the 1980 American College of Rheumatology criteria for classification of SSc,[23] confirmed by a score of >9 with the new ACR/EULAR criteria.[1] At enrolment, all patients presented neither a previous history of cardiac disease, nor electrocardiographic or echocardiographic abnormalities. No patient complained of major cardiovascular symptoms (typical angina, syncope, and dyspnoea at rest), but they were either asymptomatic or paucisymptomatic for symptoms of possible cardiovascular origin (effort dyspnoea, fatigue, and palpitations); no patient presented renal failure or any contraindication to CMR. The local Ethics Committee (Pisa, Italy, protocol number for study acceptance 2849) approved the experimental protocol. After receiving a description of the procedures and potential risks, each patient gave written informed consent.

Cardiac magnetic resonance

Study participants were examined by a 1.5-T unit (CVi, GE-Healthcare, Milwaukee, USA) using the dedicated cardiac software, eight-channel phased-array surface receiver coil and vectocardiogram triggering. Ventricular function was assessed by breath-hold steady-state free-precession cine imaging in cardiac short-axis, vertical and horizontal long-axis. In cardiac short-axis, ventricles were completely encompassed by contiguous 8-mm thick slices (with no inter-slice gap). Sequence parameters were: field-of-view: 380–400 mm, repetition/echo time: 3.2/1.6 ms, flip angle: 60°, matrix: 224 × 192, phases: 30. For the determination of the T1 value of the myocardium and blood cavity, a single mid-ventricular short-axis modified-cine inversion-recovery (MCine-IR) sequence was performed before and at fixed time intervals (5, 10, and 15 min) after the administration of a bolus of contrast agent (Gadodiamide-OMNISCAN™, 0.2 mmol/kg). MCine-IR consisted of non-selective adiabatic inversion pulse applied at the R-wave of ECG and followed by a cine segmented gradient-echo acquisition extended to the subsequent 4–6RR intervals for pre-contrast imaging or 2-RR intervals for post-contrast imaging.[24] Sequence parameters were: field-of-view: 380–400 mm, repetition/echo time: 6/2.8 ms, flip angle: 8°, matrix: 224 × 192, phases: 40. LGE imaging was performed between 10 and 20 min after contrast agent administration using a segmented T1-weighted gradient-echo inversion-recovery pulse sequence. In short-axis orientation, the LV was completely encompassed by contiguous 8-mm thick slices (with no inter-slice gap). Images were also acquired in vertical and horizontal long-axis views. Inversion time was individually adapted to suppress the signal of normal remote myocardium (220–300 ms). Sequences parameters were: field-of-view: 380–400 mm, slice thickness: 8 mm, repetition/echo time: 4.6/1.3 ms, flip angle: 20°, matrix: 256 × 192.

Image analysis

All CMR studies were analysed off-line using a workstation (Advantage Workstation, GE Healthcare, Milwaukee, USA) with a dedicated software (MASS 6.1, Medis, Leiden, Netherlands) by one experienced operator blinded to clinical data. Using the stack of short-axis cine images, left ventricular (LV) volumes, mass and global function were determined. LV volumes and mass were normalized to body surface area.[25] The presence and pattern of LGE was visually determined on post-contrast short-axis and long-axis images and, when present, LGE extent was automatically calculated on short-axis images by adopting a signal intensity threshold of >6 standard deviations (SDs) above the mean signal intensity of the remote normal myocardium, as reported in previous CMR studies in non-ischaemic cardiomyopathy.[26] For T1-mapping analysis, the signal intensity vs. time curves for the mid-ventricular septum (excluding LGE areas), the bloodpool and the skeletal muscle *(pectoralis or latissimus dorsi)* were analysed with a custom-written software (HIPPO-SW®) to determine the respective T1 and R1 values, by adopting a three-parameter mono-exponential model.[24] Of the 60 and 40 frames acquired for pre- and post-contrast analysis, respectively, only those with artefacts were excluded to keep the fitting error <10% (usually <5%). For pre- and post-contrast T1 mapping analysis, the same regions of interest were copied, pasted and eventually adjusted to compensate for possible image misalignment; when analysing the myocardium, care was taken to avoid the bloodpool; when analysing the skeletal muscle, the same muscle (the more represented between the *pectoralis or latissimus dorsi)* was analysed for each patient, and care was taken to avoid blood vessels and adipose tissue. After confirmation that a dynamic equilibrium of gadolinium between the plasma and myocardium was reached 10–15 min after contrast agent administration, R1 measurements performed at 15 min were then used to calculate the partition coefficient of gadolinium (λGd) from the slope of the linear regression line for the measured values of R1 (myocardium) vs. R1 (blood) by exploiting the linear relationship between change in relaxivity and gadolinium concentration. To determine myocardial ECV, we used the following formula: $\mathrm{ECV} = \lambda\mathrm{Gd} \times (1 - \mathrm{haematocrit})$.[17]

Statistical analysis

Continuous variables were expressed as mean ± SD or median and inter-quartile range (25th–75th percentiles), while categorical variables were expressed as frequency and percentage. Student's independent *t*-test and Mann-Whitney's test were used as appropriate to compare continuous variables. Comparison between categorical variables was performed using the χ^2, or by Fisher's exact test if the expected cell count was <5. The correlation between continuous variables was estimated by Pearson's correlation (*r*) coefficient. Two-tailed P-value < 0.05 defined statistical significance. Statistical analysis was performed by the SPSS software for Windows (20.0 release; SPSS, Chicago, IL, USA).

Results

Patient characteristics

Clinical and biohumoral data of SSc patients are given in *Table 1*. The median disease duration was 2.5 years (25th–75th percentile 1–5 years) and all patients were asymptomatic (17 patients −57%) or paucisymptomatic (13 patients, 43%, complaining of mild shortness of breath on effort). Four patients were hypertensive (13%), four presented dyslipidaemia (13%), one presented both (3%); no patient was diabetic. Only 11 patients (37%) presented an erythrocyte sedimentation rate >20 mm/h, and all patients were a relatively stable phase of disease. All patients presented normal biventricular volumes and systolic function at CMR. In particular, there was no significant difference in biventricular volumes and ejection fraction neither between SSC patients and controls (*Table 2*), nor between asymptomatic and paucisymptomatic patients.

Table 1 Clinical, biohumoral, and echocardiographic characteristics of SSc patients

Limited/diffuse cutaneous form (%)	28/2 (93/7)
Asymptomatic/symptomatic, *n* (%)	17/13 (57/43)
Modified Rodnan skin score, *n* (%)	
Score = 0	20 (67)
Score = 1	0 (0)
Score = 2	2 (6)
Score ≥ 3	8 (27)
Disease duration, years	2.5 (1–5)
Plasma creatinine, mg/dL	0.69 (0.61–0.83)
Erythrocyte sedimentation rate, mm/h	13 (9–32)
Patients with anti-Sclero-70 antibodies, *n* (%)	4 (13)
Patients with anti-centromere antibodies, *n* (%)	13 (43)
Patients with anti-nuclear antibodies, *n* (%)	24 (80)
Patients with anti-extractable nuclear antigens antibodies, *n* (%)	3 (10)
Patients with anti SSA/SSB antibodies, *n* (%)	2/2 (7/7)
Doppler estimated pulmonary artery systolic pressure, mmHg	25 (22–28)
Diastolic function *n*, (%)	
Normal	23 (77)
Impaired relaxation	6 (20)
Pseudonormal	1 (3)
Restrictive	0 (0)

Continuous variables are expressed as median and inter-quartile range (25th–75th percentiles), while categorical variables are expressed as frequency and percentage; SSA, Sjogren syndrome A; SSB, Sjogren syndrome B.

Myocardial late gadolinium enhancement and T1 mapping

LGE was absent in controls but present in 7/30 SSc patients (23%, $P < 0.01$) with a patchy pattern in three patients (involving the interventricular septal insertion points), subepicardial in two patients, mid-wall in one patient, and subendocardial/transmural in one patient. This latter finding was interpreted as a previous silent myocardial infarction, and a dipyridamole-stress nuclear scan confirmed the absence of myocardial ischaemia, making the referring clinicians decide to avoid coronary angiography. There were no differences in biventricular volumes and functions between patients with and without LGE. No patient displayed an LGE extension >10% (median LGE extension 5%, inter-quartile range 3–6%).

There was no difference in native T1 mapping values of the myocardium and bloodpool between patients and controls, but a slight non-significant difference in post-contrast T1 values (*Table 2*). In SSc patients myocardial ECV was significantly increased (30 ± 4%) than controls (28 ± 4%, $P = 0.03$) (*Figure 1*). There were no differences in myocardial ECV between patients with and without LGE (P = NS). Myocardial ECV showed no significant correlations with clinical data, symptoms, biventricular volumes, systolic, or diastolic function. An example of T1 mapping analysis of the myocardium is shown in *Figure 2*.

Skeletal muscle T1 mapping

Skeletal muscle ECV was higher in patients (23 ± 6%) than controls (18 ± 4%, $P < 0.01$) (*Figure 3*). Overall, myocardial ECV showed a significant correlation with skeletal muscle ECV ($R = 0.58$, $P < 0.001$) (*Figure 4*). On the other hand, there was no significant difference in native T1 values of the skeletal muscle between patients and controls; moreover, skeletal muscle ECV showed no significant correlations with clinical and biohumoral data, biventricular volumes, systolic, or diastolic function; even the difference in skeletal muscle ECV between asymptomatic and paucisymptomatic patients did not reach statistical significance (22 ± 5 vs. 24 ± 5%, P = NS).

Discussion

Our data show that in SSc myocardial and skeletal muscle remodelling may occur from the early stages of disease and can be identified mainly as an increased ECV at CMR. Previous studies used CMR to assess cardiac morphology and function in SSc patients. Different cardiac abnormalities have been shown, such as myocardial oedema,[27] pericardial effusion, regional and global systolic dysfunction, diastolic

Table 2 CMR parameters and ECV quantification variables in SSc patients and controls

	Patients (n = 30, all women)	Healthy controls (n = 10, all women)	*P*-value
LV end-diastolic volume (mL/m^2)	70 ± 15	74 ± 9	0.41
LV ejection fraction (%)	69 ± 7	66 ± 5	0.22
LV mass (g/m^2)	59 ± 10	58 ± 15	0.82
RV end-diastolic volume (mL/m^2)	70 ± 14	71 ± 10	0.96
RV ejection fraction (%)	65 ± 7	67 ± 7	0.57
Haematocrit	0.40 ± 0.03	0.39 ± 0.02	0.08
Glomerular filtration rate (mL/min)	91 ± 25	88 ± 13	0.64
Native myocardial T1 (ms)	790 ± 84	811 ± 89	0.52
Native bloodpool T1 (ms)	1495 ± 130	1488 ± 161	0.15
Native skeletal muscle T1 (ms)	752 ± 108	760 ± 52	0.78
Post-contrast myocardial T1 (ms)	383 ± 45	390 ± 36	0.60
Post-contrast bloodpool T1 (ms)	304 ± 53	290 ± 47	0.42
Post-contrast skeletal muscle T1 (ms)	421 ± 46	459 ± 33	0.01
Myocardial gadolinium partition coefficient (%)	51 ± 6	47 ± 7	0.02
Skeletal muscle gadolinium partition coefficient (%)	39 ± 9	30 ± 6	<0.01
Myocardial extracellular volume (%)	30 ± 4	28 ± 4	0.03
Skeletal muscle extracellular volume	23 ± 6	18 ± 4	<0.01

Variables are expressed as mean ± SD. LV, left ventricular; RV, right ventricular; LV volume, LV mass and RV volume are indexed to body surface area; the post-contrast T1 values reproduced here were acquired 15 min after contrast injection (0.2 mmol/kg Gd); the glomerular filtration rate was estimated using Cockroft-Gault formula.

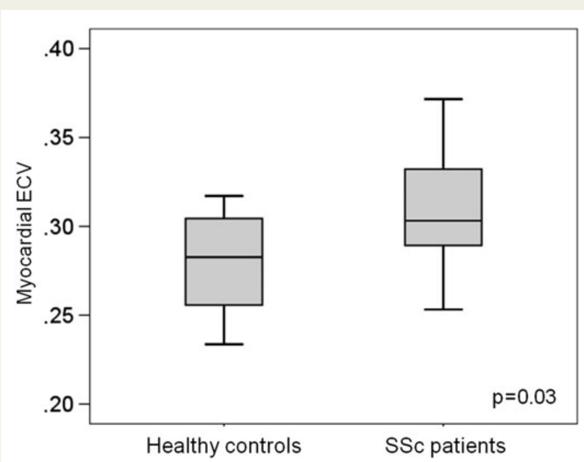

Figure 1: Myocardial ECV. Myocardial ECV was significantly increased in systemic sclerosis than controls.

dysfunction, myocardial ischemia, intramural, and patchy macroscopic fibrosis.[7,8,11–13] After the introduction of novel T1 mapping techniques, CMR has further improved its ability to characterize myocardial tissue non-invasively, providing information on myocardial oedema, interstitial fibrosis, and ECV quantification, beyond the qualitative assessment provided by traditional short-tau inversion recovery and LGE sequences.[20] Two very recent studies demonstrated myocardial interstitial remodelling in SSc patients, using T1 mapping CMR. In 33 consecutive SSc patients with normal LV function and no LGE, Thuny *et al.*[22] found an increased ECV (30.0% in SSc vs. 26.8% in controls), which correlated with left atrial volume and diastolic dysfunction. In 19 SSc patients without overt cardiovascular disease but more advanced SSc disease (mean Rodnan score 20 ± 6), Ntusi *et al.*[21] found focal fibrosis on LGE in 10 patients (53%), myocardial oedema on T2-weighted imaging, higher pre-contrast T1-mapping (1007 ± 29 vs. 958 ± 20 ms in controls), as well as ECV expansion (35.4 ± 4.8 vs. 27.6 ± 2.5%), likely representing a combination of low-grade inflammation and diffuse myocardial fibrosis. Our data represent a third independent confirmation of this early interstitial remodelling despite a completely different scanner (General Electric vs. Siemens), sequence (cine-inversion recovery vs. modified-Look-Locker sequence), and population: SSc patients in Ntusi's article were significantly sicker, with a higher Rodnan skin score, a higher prevalence of LGE, as well as much higher ECV values (∼35%); SSc patients in Thuny's article were similar to ours, as were ECV values (∼30%); in both articles, skeletal muscle remodelling, which is a possible target organ of the disease, was not analysed.

In SSc, the increased ECV could be related to intra-myocardial fibrosis, which is a frequent pattern of cardiac involvement with a rate of incidence ranging from 15 to 66%.[7,8,11–13] It is noteworthy that myocardial ECV was increased in patients with no signs of heart failure, no systolic, or diastolic dysfunction, and even in patients with no intra-myocardial LGE. On the other hand, even if biohumoral indexes of systemic inflammation were mildly increased only in a minority of patients and even if myocardial and skeletal muscle native T1 values were not higher than controls, subtle interstitial oedema, inflammation, or microvascular remodelling might represent other explanations for the increased myocardial ECV: further studies will be needed to address this point.

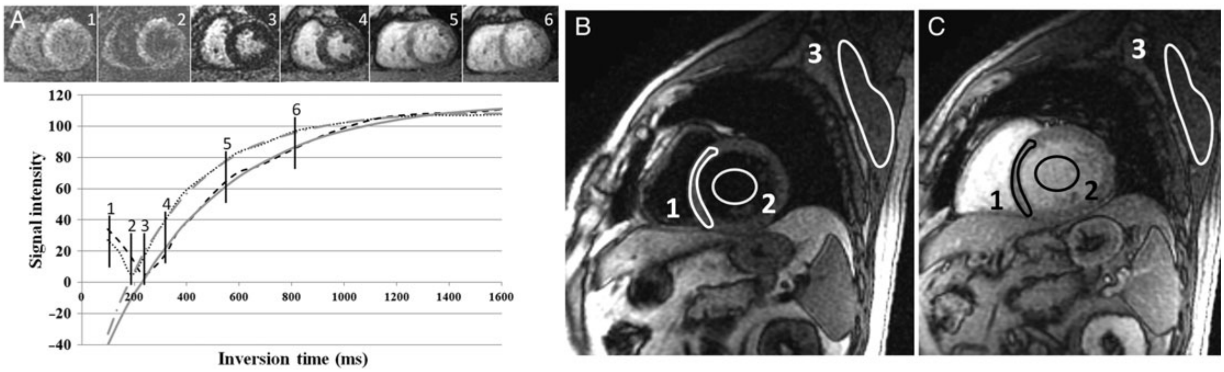

Figure 2: (A) Series of cine inversion-recovery mid-ventricular short-axis images in a SSc patient, acquired 15 min after contrast-administration (upper panel). The graph (bottom panel) shows the signal intensity of blood cavity (dotted line) and myocardium (dashed line) against the time delay after the non-slice-selective inversion pulse. The grey lines represent least-squares fits to the data points. (B and C) Short-axis mid-ventricular cine-IR image, showing where the regions of interests were placed in the myocardium (1), bloodpool (2), and skeletal muscle (3) in preconstrast (B) and post-contrast (C) analysis.

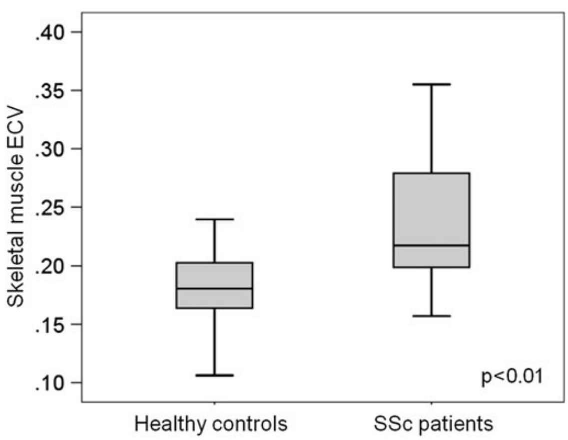

Figure 3: Skeletal muscle ECV. Skeletal muscle ECV was significantly increased in systemic sclerosis than controls.

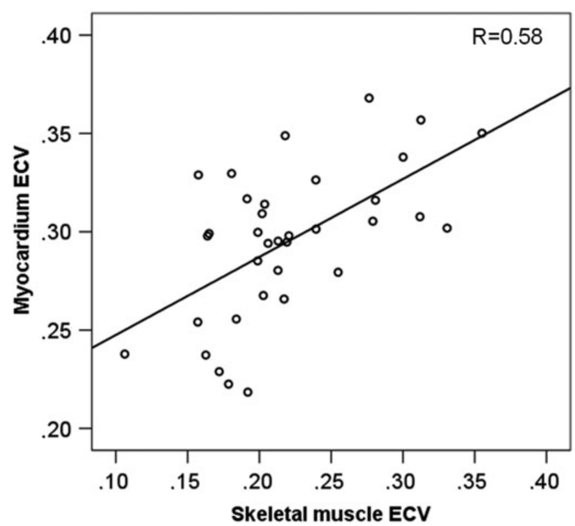

Figure 4: Correlation between myocardial ECV and skeletal muscle ECV ($R = 0.58$, $P < 0.001$).

Despite the lack of significant correlation between myocardial ECV and the extent of LGE, likely related to the exclusion of LGE areas from T1 mapping analysis, they might represent the two faces of the same phenomenon: an increased ECV might detect the earlier fibrosis deposits, not detectable by LGE. This evidence might theoretically support an early therapeutic strategy to inhibit myocardial fibrosis, for example, by targeting the renin-angiotensin-aldosterone system.[28] Fibroblast proliferation is indeed considered a leading mechanism of inappropriate collagen deposition in the myocardial interstitium, inducing reactive fibrosis.[29] In particular, interstitial myocardial fibrosis is thought to be sustained by systemic inflammation and by activation of the renin-angiotensin-aldosterone system.[30] Another pathophysiological mechanisms of myocardial fibrosis may depend on repetitive ischaemic episodes,[31] resulting from functional, and/or structural coronary microcirculation abnormalities in the presence or absence of epicardial coronary artery stenosis.[32,33] In particular, a structural vascular remodelling has been reported, consisting of perivascular fibrosis[34] and arteriolar intimal hypertrophy associated with fibrinoid necrosis of intramural coronary arteries and with intravascular coagulation.[35] Another study using intracoronary pressure wire showed a reduced resting myocardial resistance index and higher velocities, suggesting a compensatory vasodilator mechanisms with reduced coronary flow reserve.[33] In SSc patients, microvascular disease was confirmed by adenosine stress CMR[36] and by adenosine stress echocardiography,[32] and was correlated to worse prognosis. Besides a structural vascular remodelling, the occurrence of contraction band necrosis suggests that myocardial damage in SSc might be due to intermittent vascular spasm.[37]

Muscle involvement in SSc patients consists of myositis or non-inflammatory myopathy, causing weakness, and muscle atrophy.[6,38,39] The coexistence of myopathy and myocardial disease has been shown and patients with myopathy are at increased risk for cardiac dysfunction and cardiac death.[40] This relationship has been recently confirmed in an EUSTAR study showing myositis as an independent factor of heart failure.[41] This study further strengthens the close coexistence and relationship among skeletal and myocardial involvement in SSc.

Study limitations

The MCine-IR is a cine sequence that requires a relatively long processing time due to the need to trace contours in each frame, and a pixel-to-pixel T1 mapping analysis is not feasible due to the inherent cardiac motion. Moreover, the through plane motion and the inflow effects during cardiac cycle may limit the accuracy of the analysis. All these limits have been recently circumvented by novel sequences such as the modified-Look-Locker sequence (MOLLI),[42] its shortened version (ShMOLLI),[43] the saturation recovery single-shot acquisition (SASHA), and the saturation pulse prepared heart rate independent inversion recovery (SAPPHIRE), which are shorter, more reproducible, and less cumbersome than previous sequences, but are not yet commercially available for all vendors and are not completely comparable in terms of precision, accuracy, and reproducibility.[20,44,45] However, the MCine-IR sequence that we used was already validated in different clinical settings.[24,46] Our analysis was limited to the acquisition of only one mid-ventricular slice and to the analysis of the inter-ventricular septum within that slice, while SSc might affect the myocardium with a patchy pattern and whole-heart studies will be needed to address this point.

Moreover, our study was limited by a small sample size, as well as by the exclusion of patients with overt cardiac disease, which might have displayed much higher ECV values as a result of a much more evident interstitial remodelling. Another difficulty was the need to take into account the significant gender difference of the ECV between men and women.[47] For this reason, we originally measured myocardial ECV in a wider control population including 20 healthy men (age: 37 ± 16 years) besides the 10 healthy women (age: 48 ± 15 years), yielding an expected gender difference, concerning both myocardial ECV ($24 \pm 6\%$ in men, $28 \pm 4\%$ in women, $P = 0.03$), and skeletal muscle ECV ($14 \pm 3\%$ in men, $18 \pm 4\%$ in women, $P = 0.01$), confirming previous findings.[47,48] We then included only the 10 female controls, for age- and gender-matching with the SSc patients.

Because of ethical issues, the study was not designed to include endomyocardial biopsy as a tool to confirm our imaging finding, nor to investigate the relative contribution of different pathophysiological mechanisms to this remodelling (such as interstitial fibrosis, oedema, inflammation, or microvascular remodelling).

Conclusions

SSc is associated not only with replacement myocardial fibrosis as detected by LGE, but may also show early signs of interstitial myocardial remodelling, supported by an increased ECV. This evidence is paralleled by an increased ECV in the skeletal muscle. Both myocardial and skeletal muscle interstitial remodelling may represent early markers of cardiac involvement that are present before ventricular dysfunction and symptoms. Indeed, they may help to identify high-risk patients to be submitted to a targeted therapy. Moreover, further studies are needed to investigate the histopathological nature of this early interstitial remodelling (collagen deposition, oedema, or inflammation) and to provide definitive evidence of the coexistence of cardiac and musculoskeletal involvement.

Acknowledgements

The authors thank Mrs Claudia Venneri and Claudia Santarlasci for the secretarial support.

Conflict of interest: none declared.

References

1. van den Hoogen F, Khanna D, Fransen J, Johnson SR, Baron M, Tyndall A*et al.* 2013 classification criteria for systemic sclerosis: an American College of Rheumatology/European League against Rheumatism Collaborative Initiative. *Arthritis Rheum* 2013;**65**:2737–47.
2. Barnes J, Mayes MD. Epidemiology of systemic sclerosis: incidence, prevalence, survival, risk factors, malignancy, and environmental triggers. *Curr Opin Rheumatol* 2012;**24**:165–70.
3. Ferri C, Giuggioli D, Sebastiani M, Colaci M, Emdin M. Heart involvement and systemic sclerosis. *Lupus* 2005;**14**:702–7.
4. Desai CS, Lee DC, Shah SJ. Systemic sclerosis and the heart: current diagnosis and management. *Curr Opin Rheumatol* 2011;**23**:545–54.
5. Ioannidis JPA, Vlachoyiannopoulos PG, Haidich A-B, Medsger TA, Lucas M, Michet CJ *et al.* Mortality in systemic sclerosis: an international meta-analysis of individual patient data. *Am J Med* 2005;**118**:2–10.
6. Ranque B, Authier F-J, Berezne A, Guillevin L, Mouthon L. Systemic sclerosis-associated myopathy. *Ann N Y Acad Sci* 2007;**1108**:268–82.
7. Tzelepis GE, Kelekis NL, Plastiras SC, Mitseas P, Economopoulos N, Kampolis C *et al.* Pattern and distribution of myocardial fibrosis in systemic sclerosis: a delayed enhanced magnetic resonance imaging study. *Arthritis Rheum* 2007;**56**:3827–36.
8. Hachulla A-L, Launay D, Gaxotte V, de Groote P, Lamblin N, Devos P *et al.* Cardiac magnetic resonance imaging in systemic sclerosis: a cross-sectional observational study of 52 patients. *Ann Rheum Dis* 2009;**68**:1878–84.
9. Moon J, Coghlan JG, Pennell DJ. Systemic sclerosis involving the heart. *Heart* 2001;**86**:308.
10. Plastiras SC, Kelekis N, Tzelepis GE. Magnetic resonance imaging for the detection of myocardial fibrosis in scleroderma. *N Engl J Med* 2006;**354**:2194–6.
11. Nassenstein K, Breuckmann F, Huger M, Ladd SC, Schlosser T, Kreuter A *et al.* Detection of myocardial fibrosis in systemic sclerosis by contrast-enhanced magnetic resonance imaging. *Rofo* 2008;**180**:1054–60.
12. Di Cesare E, Battisti S, Di Sibio A, Cipriani P, Giacomelli R, Liakouli V *et al.* Early assessment of sub-clinical cardiac involvement in systemic sclerosis (SSc) using delayed enhancement cardiac magnetic resonance (CE-MRI). *Eur J Radiol* 2013;**82**:e268–73.
13. Mavrogeni S, Bratis K, van Wijk K, Stavropoulos E, Hautemann D, Reiber JHC *et al.* Myocardial perfusion-fibrosis pattern in systemic sclerosis assessed by cardiac magnetic resonance. *Int J Cardiol* 2012;**159**:e56–8.
14. Ferreira VM, Piechnik SK, Dall'Armellina E, Karamitsos TD, Francis JM, Ntusi N *et al.* T(1) mapping for the diagnosis of acute myocarditis using CMR: comparison to T2-weighted and late gadolinium enhanced imaging. *JACC Cardiovasc Imaging* 2013;**6**:1048–58.
15. Ferreira VM, Piechnik SK, Dall'Armellina E, Karamitsos TD, Francis JM, Choudhury RP *et al.* Non-contrast T1-mapping detects acute myocardial edema with high diagnostic accuracy: a comparison to T2-weighted cardiovascular magnetic resonance. *J Cardiovasc Magn Reson* 2012;**14**:42.
16. Bull S, White SK, Piechnik SK, Flett AS, Ferreira VM, Loudon M *et al.* Human non-contrast T1 values and correlation with histology in diffuse fibrosis. *Heart* 2013;**99**:932–7.
17. Flett AS, Hayward MP, Ashworth MT, Hansen MS, Taylor AM, Elliott PM *et al.* Equilibrium contrast cardiovascular magnetic resonance for the measurement of diffuse myocardial fibrosis: preliminary validation in humans. *Circulation* 2010;**122**:138–44.
18. White SK, Sado DM, Fontana M, Banypersad SM, Maestrini V, Flett AS *et al.* T1 mapping for myocardial extracellular volume measurement by CMR: bolus only versus primed infusion technique. *JACC Cardiovasc Imaging* 2013;**6**:955–62.
19. Fontana M, White SK, Banypersad SM, Sado DM, Maestrini V, Flett AS *et al.* Comparison of T1 mapping techniques for ECV quantification. Histological validation and reproducibility of ShMOLLI versus multibreath-hold T1 quantification equilibrium contrast CMR. *J Cardiovasc Magn Reson* 2012;**14**:88.

20. Moon JC, Messroghli DR, Kellman P, Piechnik SK, Robson MD, Ugander M *et al.* Myocardial T1 mapping and extracellular volume quantification: a Society for Cardiovascular Magnetic Resonance (SCMR) and CMR Working Group of the European Society of Cardiology consensus statement. *J Cardiovasc Magn Reson* 2013;**15**:92.
21. Ntusi NA, Piechnik SK, Francis JM, Ferreira VM, Rai AB, Matthews PM *et al.* Subclinical myocardial inflammation and diffuse fibrosis are common in systemic sclerosis – a clinical study using myocardial T1-mapping and extracellular volume quantification. *J Cardiovasc Magn Reson* 2014;**16**:21.
22. Thuny F, Lovric D, Schnell F, Bergerot C, Ernande L, Cottin V *et al.* Quantification of myocardial extracellular volume fraction with cardiac MR imaging for early detection of left ventricle involvement in systemic sclerosis. *Radiology* 2014;**271**:373–80.
23. Preliminary criteria for the classification of systemic sclerosis (scleroderma). Subcommittee for scleroderma criteria of the American Rheumatism Association Diagnostic and Therapeutic Criteria Committee. *Arthritis Rheum* 1980;**23**:581–90.
24. Milanesi M, Barison A, Positano V, Masci PG, De Marchi D, Marinelli L *et al.* Modified cine inversion recovery pulse sequence for the quantification of myocardial T1 and gadolinium partition coefficient. *J Magn Reson Imaging* 2013;**37**:109–18.
25. Maceira A, Prasad S. Normalized left ventricular systolic and diastolic function by steady state free precession cardiovascular magnetic resonance. *J Cardiovasc Magn Reson* 2006;**8**:417–26.
26. Bondarenko O, Beek AM, Hofman MBM, Kühl HP, Twisk JWR, van Dockum WG *et al.* Standardizing the definition of hyperenhancement in the quantitative assessment of infarct size and myocardial viability using delayed contrast-enhanced CMR. *J Cardiovasc Magn Reson* 2005;**7**:481–5.
27. Pingitore A, Guiducci S, Conforti ML, De Marchi D, Gargani L, Moggi-Pignone A *et al.* Early detection of myocardial and pulmonary oedema with MRI in an asymptomatic systemic sclerosis patient: successful recovery with pulse steroid. *Rheumatology (Oxford)* 2013;**52**:1920–1.
28. Díez J, Querejeta R, López B, González A, Larman M, Martínez Ubago JL. Losartan-dependent regression of myocardial fibrosis is associated with reduction of left ventricular chamber stiffness in hypertensive patients. *Circulation* 2002;**105**:2512–7.
29. Fleischmajer R, Perlish JS, Duncan M. Scleroderma. A model for fibrosis. *Arch Dermatol* 1983;**119**:957–62.
30. Guiducci S, Fatini C, Rogai V, Cinelli M, Sticchi E, Abbate R *et al.* Angiotensin-converting enzyme in systemic sclerosis: from endothelial injury to a genetic polymorphism. *Ann N Y Acad Sci* 2006;**1069**:10–9.
31. Meune C, Vignaux O, Kahan A, Allanore Y. Heart involvement in systemic sclerosis: evolving concept and diagnostic methodologies. *Arch Cardiovasc Dis* 2010;**103**:46–52.
32. Vacca A, Montisci R, Garau P, Siotto P, Piga M, Cauli A *et al.* Prognostic impact of coronary microcirculation abnormalities in systemic sclerosis: a prospective study to evaluate the role of non-invasive tests. *Arthritis Res Ther* 2013;**15**:R8.
33. Pintér T, Faludi R, Magyari B, Vorobcsuk A, Kumánovics G, Minier T *et al.* Mechanism of coronary flow reserve reduction in systemic sclerosis: insight from intracoronary pressure wire studies. *Rheumatology (Oxford)* 2011;**50**:781–8.
34. Fernandes F, Ramires FJA, Arteaga E, Ianni BM, Bonfá ESDO, Mady C. Cardiac remodeling in patients with systemic sclerosis with no signs or symptoms of heart failure: an endomyocardial biopsy study. *J Card Fail* 2003;**9**:311–7.
35. James TN. De subitaneis mortibus. VIII. Coronary arteries and conduction system in scleroderma heart disease. *Circulation* 1974;**50**:844–56.
36. Kobayashi H, Yokoe I, Hirano M, Nakamura T, Nakajima Y, Fontaine KR *et al.* Cardiac magnetic resonance imaging with pharmacological stress perfusion and delayed enhancement in asymptomatic patients with systemic sclerosis. *J Rheumatol* 2009;**36**:106–12.
37. Bulkley BH, Ridolfi RL, Salyer WR, Hutchins GM. Myocardial lesions of progressive systemic sclerosis. A cause of cardiac dysfunction. *Circulation* 1976;**53**:483–90.
38. Olsen NJ, King LE, Park JH. Muscle abnormalities in scleroderma. *Rheum Dis Clin North Am* 1996;**22**:783–96.
39. Schade L, Paiva EDS, Müller C de S. Skeletal and cardiac muscles involvement in systemic sclerosis. *Rev Bras Reumatol* 2011;**51**:309–10, 313.
40. Follansbee WP, Zerbe TR, Medsger TA. Cardiac and skeletal muscle disease in systemic sclerosis (scleroderma): a high risk association. *Am Heart J* 1993;**125**:194–203.
41. Allanore Y, Meune C, Vonk MC, Airo P, Hachulla E, Caramaschi P *et al.* Prevalence and factors associated with left ventricular dysfunction in the EULAR Scleroderma Trial and Research group (EUSTAR) database of patients with systemic sclerosis. *Ann Rheum Dis* 2010;**69**:218–21.
42. Messroghli DR, Plein S, Higgins DM, Walters K, Jones TR, Ridgway JP *et al.* Human myocardium: single-breath-hold MR T1 mapping with high spatial resolution—reproducibility study. *Radiology* 2006;**238**:1004–12.
43. Piechnik SK, Ferreira VM, Dall'Armellina E, Cochlin LE, Greiser A, Neubauer S *et al.* Shortened Modified Look-Locker Inversion recovery (ShMOLLI) for clinical myocardial T1-mapping at 1.5 and 3 T within a 9 heartbeat breathhold. *J Cardiovasc Magn Reson* 2010;**12**:69.
44. Roujol S, Weingärtner S, Foppa M, Chow K, Kawaji K, Ngo LH *et al.* Accuracy, precision, and reproducibility of four T1 mapping sequences: a head-to-head comparison of MOLLI, ShMOLLI, SASHA, and SAPPHIRE. *Radiology* 2014; DOI: http://dx.doi.org/10.1148/radiol.14140296.
45. Nacif MS, Turkbey EB, Gai N, Nazarian S, van der Geest RJ, Noureldin RA *et al.* Myocardial T1 mapping with MRI: comparison of look-locker and MOLLI sequences. *J Magn Reson Imaging* 2011;**34**:1367–73.
46. Fontana M, Barison A, Botto N, Panchetti L, Ricci G, Milanesi M *et al.* CMR-verified interstitial myocardial fibrosis as a marker of subclinical cardiac involvement in LMNA mutation carriers. *JACC Cardiovasc Imaging* 2013;**6**:124–6.
47. Sado D, Flett A, Banypersad S, White S, Maestrini V, Quarta G *et al.* Cardiovascular magnetic resonance measurement of myocardial extracellular volume in health and disease. *Heart* 2012;**98**:1436–41.
48. Liu C-Y, Liu Y-C, Wu C, Armstrong A, Volpe GJ, van der Geest RJ *et al.* Evaluation of age-related interstitial myocardial fibrosis with cardiac magnetic resonance contrast-enhanced T1 mapping: MESA (Multi-Ethnic Study of Atherosclerosis). *J Am Coll Cardiol* 2013;**62**:1280–7.